Journal of Solid State Chemistry 184 (2011) 2353–2359

Contents lists available at ScienceDirect

Journal of Solid State Chemistry

journal homepage: www.elsevier.com/locate/jssc

Effect of Cr and Mn ions on the structure and magnetic properties of $GaFeO_3$: Role of the substitution site

Rana Saha, Ajmala Shireen, Sharmila N. Shirodkar, Umesh V. Waghmare, A. Sundaresan, C.N.R. Rao *

Chemistry and Physics of Materials Unit, New Chemistry Unit, Theoretical Science Unit and International Centre for Materials Science, Jawaharlal Nehru Centre for Advanced Scientific Research, Jakkur P.O., Bangalore 560064, India

ARTICLE INFO

Article history:
Received 12 April 2011
Received in revised form
4 July 2011
Accepted 6 July 2011
Available online 14 July 2011

Keywords:
$GaFeO_3$
Magnetic properties
Site-specificity
DFT calculations

ABSTRACT

Effect of substitution of Cr and Mn in the Fe and Ga sites of $GaFeO_3$ on the structural parameters and magnetic properties has been investigated by preparing $GaFe_{1-x}Cr_x(Mn_x)O_3$ and $Ga_{1-x}Cr_x(Mn_x)FeO_3$ starting with appropriate oxide precursors. It is shown that, starting with Cr or Mn substituted Ga_2O_3, one obtains $Ga_{1-x}Cr_x(Mn_x)FeO_3$, while reaction of Cr or Mn substituted α-Fe_2O_3 with Ga_2O_3 yields $GaFe_{1-x}Cr_x(Mn_x)O_3$. The structural parameters and magnetic properties vary significantly with the substitution site of Cr showing a large decrease in the unit cell parameters as well as the T_C and other magnetic properties when the substitution is at the octahedral Fe (1, 2) site. Substitution of Cr at the octahedral Ga2 site results in marginal changes. Substitution of Mn in the Ga and Fe sites also show differences although the changes themselves are much smaller. First-principles calculations confirm such site-specificity and show how Cr substitution affects the properties differently when substituted at the Ga2 and Fe1 sites.

1. Introduction

Both $AlFeO_3$ and $GaFeO_3$ crystallize in the non-centrosymmetric chiral space group ($Pna2_1$) with an orthorhombic structure [1,2]. They are ferrimagnetic [3,4], with interesting dielectric properties [5]. The Curie temperature (T_C) of $GaFeO_3$ is 210 K. There are two sites for Fe and two for Ga in $GaFeO_3$, with Fe1, Fe2 and Ga2 in the octahedral environment (see Fig. 1). The octahedra share edges whereas the tetrahedra (Ga1) share oxygen at the corners. There is no edge-sharing between octahedra and tetrahedra. Disorder plays an important role in determining the properties of $GaFeO_3$ and there is indeed some occupancy of the Ga sites by the Fe ions. Thus, the occupancy factors of the Fe1, Fe2, Al2 and Al1 sites in $AlFeO_3$ are estimated to be 0.83, 0.81, 0.26 and 0.14, respectively, from neutron diffraction studies [6]. We were interested in studying the effect of chromium and manganese substitution on the magnetic properties of $GaFeO_3$ since it is known that both the transition metal ions can be incorporated in Fe_2O_3 and Ga_2O_3 [7–10]. In particular, we wanted to examine site specific effects of Cr and Mn substitution. With this purpose, we prepared the Cr and Mn substituted $GaFeO_3$ samples by reacting Ga_2O_3 substituted with the desired proportion of Cr or Mn with α-Fe_2O_3 as well as by interacting α-Fe_2O_3 substituted with the desired proportion of Cr or Mn with Ga_2O_3 instead of mixing the three parent metal oxides together [11,12]. The method of preparation employed by us was expected to give rise to preferential substitution of Cr or Mn ions in the Fe (1, 2) or the Ga2 site. The present study has shown marked differences in the structural parameters and magnetic properties of the $GaFeO_3$ samples prepared by us starting with Cr (Mn) substituted Ga_2O_3 and Cr (Mn) substituted α-Fe_2O_3, indicating that substitution occurs specifically in Ga2 site and Fe (1, 2) site, respectively. We have carried first-principles calculations to throw light on the above results. The calculations clearly show how substitution at the Ga2 and Fe1 sites would have different effects on the structural parameters and magnetic properties of $GaFeO_3$, thereby lending support to the conclusions from experimental studies.

2. Experimental

Chromium and manganese substituted $GaFeO_3$ were prepared by the following two methods. α-Fe_2O_3 was substituted by appropriate quantities of Cr or Mn by calcining stoichiometric mixtures of Fe_2O_3 (Aldrich, 99.98%) and Cr_2O_3 (Aldrich, 99.9%) or Mn_2O_3 (Aldrich, 99.0%) at 1000 °C for 12 h. The XRD patterns of $(Fe_{1-x}M_x)_2O_3$ (M=Cr, Mn) could be indexed on the basis of the rhombohedral structure of α-Fe_2O_3 (Table 1). The pellets were ground again and mixed with stoichiometric amounts of β-Ga_2O_3 (Aldrich, 99.99%) and sintered at 1300 °C for 12 h. Thus, $GaFe_{1-x}M_xO_3$ (M=Cr, Mn; x=0.05, 0.1) compositions where the Fe site was substituted by Cr or Mn were obtained. In the second

* Corresponding author. Fax: +91 80 22082766.
E-mail address: cnrrao@jncasr.ac.in (C.N.R. Rao).

0022-4596/$ - see front matter © 2011 Elsevier Inc. All rights reserved.
doi:10.1016/j.jssc.2011.07.006

procedure, Ga_2O_3 was substituted by Cr or Mn by mixing stoichiometric amounts of Ga_2O_3 and Cr_2O_3 or Mn_2O_3. This mixture was then calcined at 1100 °C (12 h). The XRD pattern of $(Ga_{1-x}M_x)_2O_3$ (M=Cr, Mn) could be indexed on the basis of monoclinic structure of β-Ga_2O_3 (Table 1). The pellets were ground again and mixed with stoichiometric amounts of α-Fe_2O_3 and sintered at 1300 °C for 12 h. This yielded $Ga_{1-x}M_xFeO_3$ (M=Cr, Mn; x=0.05, 0.1) compositions where Cr or Mn ions were substituted at the Ga site.

X-ray diffraction patterns of the oxides were recorded with a Bruker D8 Advance X-ray diffractometer to confirm the phase purity. Structural data were analyzed with a software package Fullprof. Magnetic measurements were carried out with a vibrating sample magnetometer in the Physical Property Measurement System (PPMS) under zero-field-cooled (ZFC) and field-cooled (FC) conditions in the temperature range of 10–350 K under a magnetic field of 100 Oe. Magnetic hysteresis was recorded at a temperature of 5 K with field reaching a value of 60 kOe.

3. Results and discussion

Crystal structure data of all the $GaFe_{1-x}Cr_x(Mn_x)O_3$ and $Ga_{1-x}Cr_x(Mn_x)FeO_3$ compositions are summarized in Table 2. In Fig. 2 we show typical X-ray diffraction patterns of $GaFe_{0.9}Cr_{0.1}O_3$ and $Ga_{0.9}Cr_{0.1}FeO_3$ compositions along with the profile fits to show how both the oxides possess the same orthorhombic crystal structure. In Fig. 3 we show the variation of unit cell parameters of $GaFe_{1-x}Cr_xO_3$ and $Ga_{1-x}Cr_xFeO_3$ with composition. We readily see that the lattice parameters and the unit cell volume are more markedly affected by Cr substitution in $GaFe_{1-x}Cr_xO_3$ compared to those of $Ga_{1-x}Cr_xFeO_3$. The lattice parameters and unit cell volume decrease in both the series but the decrease is marginal in $Ga_{1-x}Cr_xFeO_3$. The unit cell volume of $GaFe_{1-x}Cr_xO_3$ decreases from 417.2 Å^3 (x=0.0) to 414.2 Å^3 (x=0.2) compared to $Ga_{1-x}Cr_xFeO_3$, which has a unit cell volume close to that of $GaFeO_3$. These changes are consistent with the radius of octahedral Cr^{3+} relative to Fe^{3+} and Ga^{3+}, the radius of Cr^{3+} being considerably smaller than that of Fe^{3+}. In order to establish that Cr^{3+} has gone into the Ga site in the $Ga_{1-x}Cr_xFeO_3$ series of compounds we have carried out detailed analysis of the XRD data for the x=0.1 composition. For this purpose, we fixed all the occupancies as X-ray cannot differentiate these elements of close atomic numbers. The occupancies were fixed based on our previous neutron diffraction results. The thermal parameters were refined iteratively while placing the dopant atoms at different (Ga and Fe) sites and found large thermal parameters when the atoms were placed at Fe sites. We show the results of the refinement in Table 3 to indicate that the proposed cation distribution is consistent with the diffraction data, but due to similar scattering powers of the cations the diffraction data is not actually very sensitive to the cation distribution. The differences observed in the structural parameters and magnetic properties of $GaFe_{1-x}Cr_xO_3$ and $Ga_{1-x}Cr_xFeO_3$ also show that we have achieved Cr substitution in different sites.

$GaFe_{1-x}Cr_xO_3$ exhibits ferrimagnetic T_C values of 192, 170 and 110 K for x=0.05, 0.1 and 0.2, respectively, compared with a T_C of 210 K in the case of $GaFeO_3$. We show typical magnetization plots of $GaFe_{1-x}Cr_xO_3$ and $Ga_{1-x}Cr_xFeO_3$ (x=0.1) in Fig. 4. We see from Fig. 5(a) that T_C decreases significantly with increase in x in $GaFe_{1-x}Cr_xO_3$. All these compounds show magnetic hysteresis at 5 K and the values of maximum magnetization (M_S) and remanant magnetization (M_R) in $GaFe_{1-x}Cr_xO_3$ for x=0.05(0.1) are 16.4(13.5) and 8.4(6.5) emu/g, respectively. The maximum

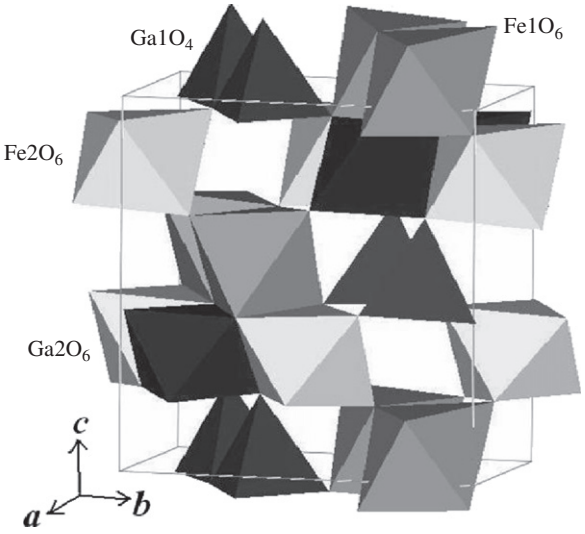

Fig. 1. The crystal structure of $GaFeO_3$.

Table 2
Crystallographic data of $GaFe_{1-x}M_xO_3$ and $Ga_{1-y}M_yFeO_3$ (M=Cr, Mn).

	% substitution	a (Å)	b (Å)	c (Å)	χ^2 (%)	R_{Bragg} (%)
$GaFe_{1-x}M_xO_3$ (space group: $Pna2_1$, orthorhombic)						
x (Cr)	0	5.0814 (2)	8.7436 (3)	9.3910 (2)	2.30	2.74
	5	5.0778 (0)	8.7335 (1)	9.3814 (1)	2.11	1.50
	10	5.0762 (1)	8.7307 (1)	9.3765 (1)	2.72	1.74
	20	5.0712 (1)	8.7222 (1)	9.3640 (1)	2.93	1.67
x (Mn)	5	5.0802 (1)	8.7346 (1)	9.3828 (1)	2.02	2.26
	10	5.0832 (1)	8.7379 (1)	9.3848 (1)	1.79	1.42
$Ga_{1-y}M_yFeO_3$ (space group: $Pna2_1$, orthorhombic)						
y (Cr)	5	5.0786 (1)	8.7363 (1)	9.3856 (1)	2.73	1.58
	10	5.0795 (1)	8.7386 (1)	9.3870 (1)	2.07	1.58
y (Mn)	5	5.0821 (6)	8.7395 (1)	9.3878 (1)	2.41	2.09
	10	5.0833 (7)	8.7412 (1)	9.3892 (1)	2.75	2.01

Table 1
Crystallographic data of precursor oxides.

	% substitution	a (Å)	b (Å)	c (Å)	χ^2 (%)	R_{Bragg} (%)
$(Fe_{1-x}M_x)_2O_3$ (space group: $R\bar{3}c$, rhombohedral)						
x (Cr)	10	5.0309 (4)		13.7167 (13)	2.41	1.71
x (Mn)	10	5.0351 (5)		13.7392 (18)	1.70	2.30
$(Ga_{1-y}M_y)_2O_3$ (space group: $C2/m$, monoclinic)						
y (Cr)	10	12.2459 (7)	3.0410 (2)	5.8114 (3)	3.57	0.62
y (Mn)	10	12.2894 (13)	3.0505 (2)	5.8320 (5)	3.07	0.76

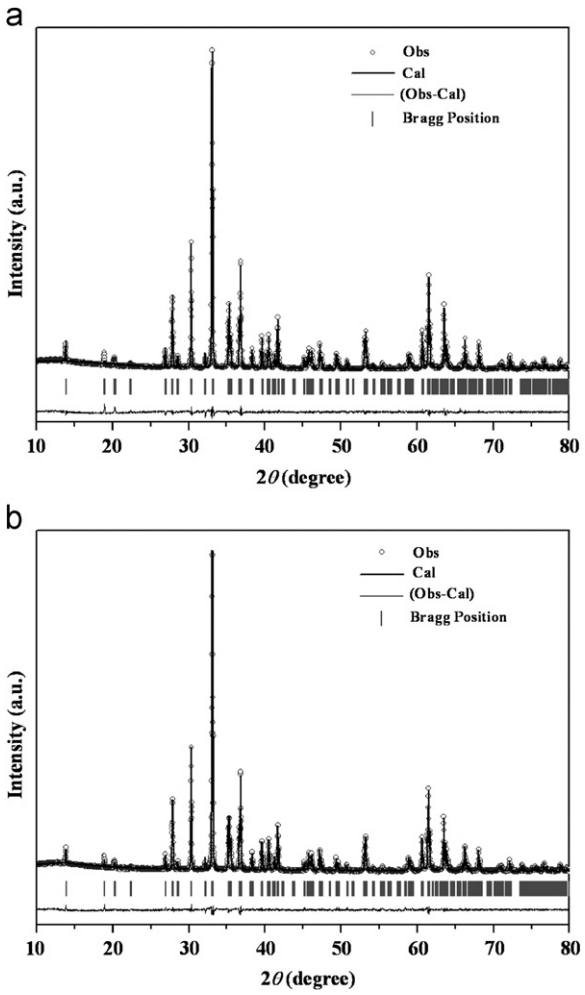

Fig. 2. XRD patterns of (a) $GaFe_{0.9}Cr_{0.1}O_3$ and (b) $Ga_{0.9}Cr_{0.1}FeO_3$ along with profile fits, difference patterns and Bragg positions.

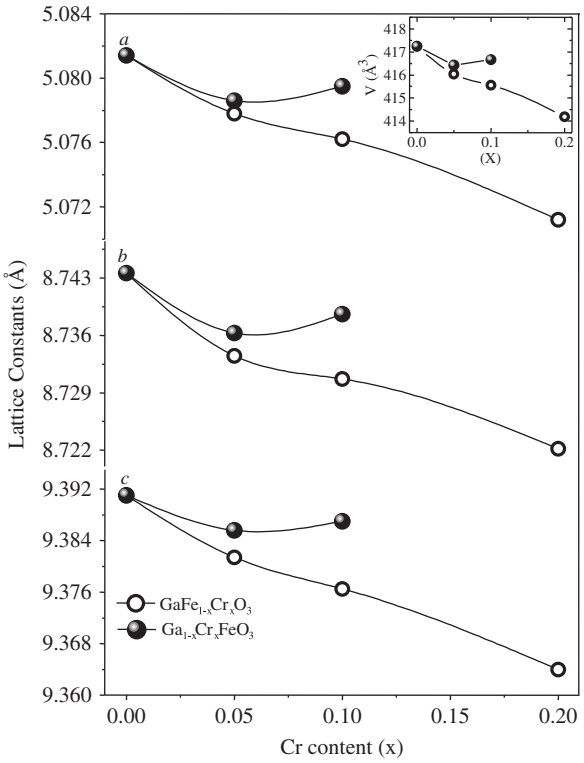

Fig. 3. Variation of lattice constants in $GaFe_{1-x}Cr_xO_3$ and $Ga_{1-x}Cr_xFeO_3$ with Cr content at 300 K obtained from XRD data. Variation of unit cell volume is shown in the inset.

magnetization at 5 K also decreases with increase in x as shown in Fig. 5(b). Magnetization data of $Ga_{1-x}Cr_xFeO_3$ (x=0.05, 0.1) show only a small variation in T_C with increase in x in this series of oxides as can be seen from Fig. 5(a). The values of maximum magnetization and remanant magnetization in $Ga_{1-x}Cr_xFeO_3$ for x=0.05(0.1) are 19.1(19.7) and 9.8(10) emu/g, respectively. We see negligible changes in M_S and M_R with x in $Ga_{1-x}Cr_xFeO_3$ (see Fig. 5b). The important result from the study of Cr substitution in $GaFeO_3$ is that Cr substitution in the Fe site in $GaFe_{1-x}Cr_xO_3$ markedly affects the structural parameters as well as the magnetic properties while substitution of Cr at the Ga site has marginal effects. It must be noted that the magnetization data of Cr-substituted $GaFeO_3$ prepared from a three-component mixture of Ga_2O_3, Fe_2O_3 and Cr_2O_3 are entirely different. The T_C values and the unit cell parameters are also different [11]. Thus, there is negligible change in the unit cell volume even when x=0.15 and the T_C values are much lower than those observed here.

We have carried out an investigation on Mn-substituted $GaFeO_3$ samples. In Table 2 we have summarized the crystal structure data of these oxides. We show typical X-ray diffraction patterns of $GaFe_{1-x}Mn_xO_3$ and $Ga_{1-x}Mn_xFeO_3$ with x=0.1 along with the profile fits in Fig. 6. Fig. 7 shows the variation of unit cell parameters and volume of $GaFe_{1-x}Mn_xO_3$ and $Ga_{1-x}Mn_xFeO_3$ with x. The changes in the unit cell parameters are marginal in the Mn substituted $GaFeO_3$, considering that Fe^{3+} and Mn^{3+} have the same radii. It is difficult however, to quantitatively interpret the observed changes. We have carried out analysis of the XRD data of $Ga_{0.9}Mn_{0.1}FeO_3$ and show the results of the refinement in Table 4.

Typical magnetization plots for $GaFe_{1-x}Mn_xO_3$ and $Ga_{1-x}Mn_xFeO_3$ (x=0.1) are shown in Fig. 8. The T_C value decreases to 162 K in $GaFe_{1-x}Mn_xO_3$ (x=0.1), but the value is around 201 K in $Ga_{1-x}Mn_xFeO_3$ (x=0.1) as can be seen from Fig. 9(a). The maximum magnetization and remanent magnetization show marked decrease with increase in Mn content in the Fe site (Fig. 9b). From the magnetization data of $Ga_{1-x}Mn_xFeO_3$ (x=0.1), we find that the changes in the magnetization value and in T_C are not large with change in x. Interestingly, we observe that the T_C decreases to 197 K for x=0.05 but increases slightly to 201 K with increase in the Mn content (x=0.1). The magnetic properties and structural parameters of Mn substituted $GaFeO_3$ prepared from the three component oxides [12] are quite different from those reported here. The data in Ref. [12] show wide variation depending on the method of preparation. Slight changes in the oxidation state of Mn can also be responsible for such observations.

The results on $GaFe_{1-x}Cr_x(Mn_x)O_3$ and $Ga_{1-x}Cr_x(Mn_x)FeO_3$ (x=0.05, 0.1) found by us establish that the method of preparation employed by us has enabled site-selective substitution. The changes in structural parameters and magnetic properties with x corroborate the occurrence of specific site effects. We also note that the decrease in T_C and other properties of $GaFe_{1-x}Cr_xO_3$ with increase in x parallels the decrease in unit cell volume. Such a decrease in T_C with unit cell volume has been documented in rare earth chromites.

We have studied the effect of Cr doping at Fe1, Fe2, Ga1 and Ga2 sites, taking the concentration of doping to be one Cr per unit cell (i.e. 12.5%), by first-principles calculations. Our calculations are based on density functional theory (DFT) with a spin-density dependent exchange correlation energy functional that includes generalized gradient corrections (Perdew Wang 91 (PW 91) form

Table 3
Results of structure refinement of $Ga_{0.9}Cr_{0.1}FeO_3$ at 300 K.

$Ga_{0.9}Cr_{0.1}FeO_3$ (300 K)					
Space group: *Pna*2$_1$ (Orthorhombic), a=5.0795 (1) Å , b=8.7386 (1) Å and c=9.3870 (1) Å					
Atoms	*x/a*	*y/b*	*z/c*	B_{iso}	Occ.
Fe1/Ga3	0.1968 (10)	0.1507 (8)	0.5857 (4)	0.95 (11)	0.65 (0)/0.35 (0)
Fe2/Ga4	0.6741 (6)	0.0335 (3)	0.7939 (7)	0.75 (6)	0.70 (0)/0.30 (0)
Ga1/Fe3	0.1742 (8)	0.1543 (8)	0.0000 (0)	1.60 (10)	0.91 (0)/0.09 (0)
Ga2/Fe4/Cr	0.8148 (6)	0.1632 (4)	0.3090 (5)	0.25 (7)	0.26 (0)/0.554 (0)/0.200 (0)
O1	0.984 (3)	0.324 (2)	0.423 (1)	0.51 (8)	1.000 (0)
O2	0.531 (2)	0.485 (2)	0.428 (1)	0.51 (8)	1.000 (0)
O3	0.655 (3)	0.005 (1)	0.208 (1)	0.51 (8)	1.000 (0)
O4	0.156 (3)	0.156 (2)	0.200 (0)	0.51 (8)	1.000 (0)
O5	0.867 (3)	0.160 (2)	0.671 (1)	0.51 (8)	1.000 (0)
O6	0.526 (3)	0.163 (2)	0.941 (1)	0.51 (8)	1.000 (0)
χ^2	2.20%				
R_{Bragg}	8.09%				

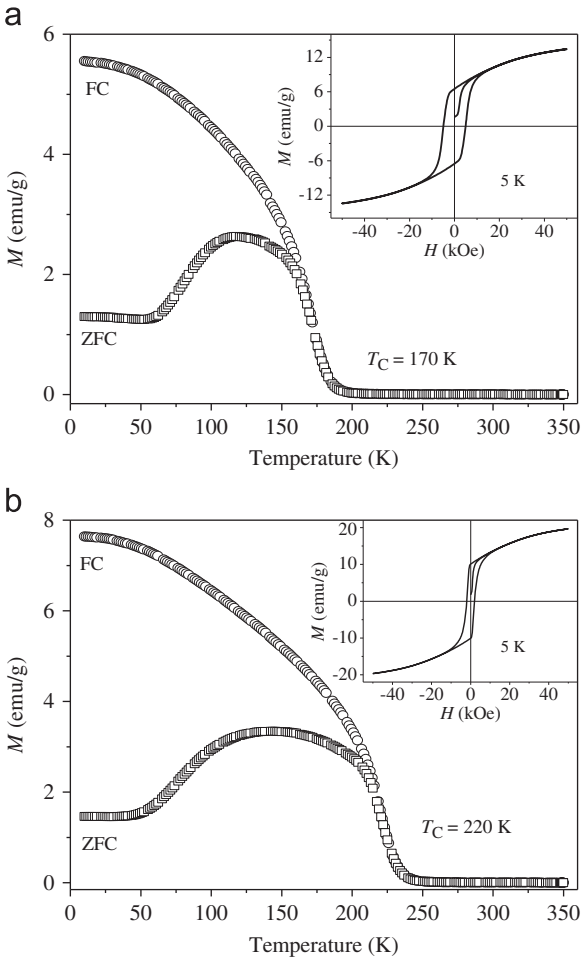

Fig. 4. Temperature-dependent magnetization of (a) $GaFe_{0.9}Cr_{0.1}O_3$ and (b) $Ga_{0.9}Cr_{0.1}FeO_3$ under field-cooled (FC) and zero-field-cooled (ZFC) conditions. Magnetic hysteresis at 5 K is shown in the inset.

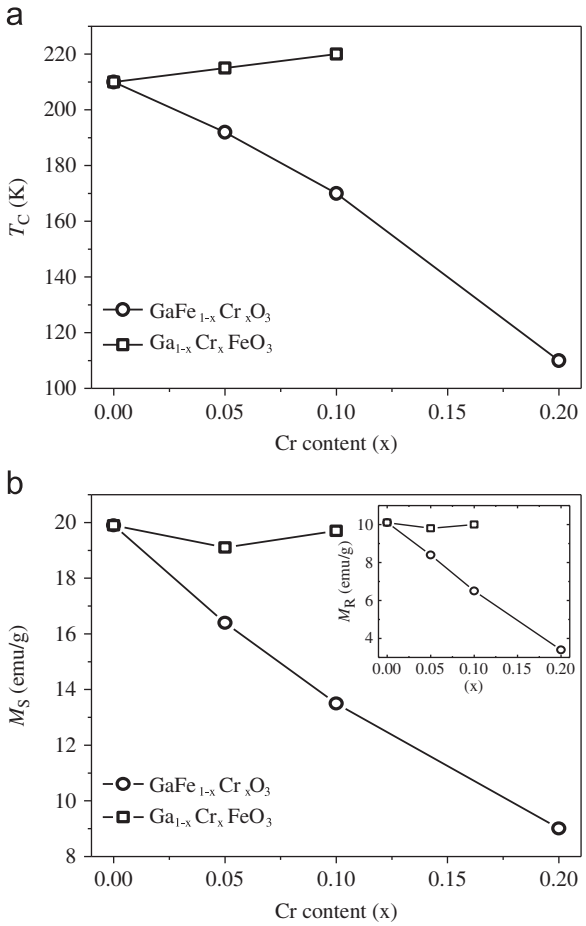

Fig. 5. (a) Variation of the Curie temperature (T_C) with Cr concentration in $GaFe_{1-x}Cr_xO_3$and $Ga_{1-x}Cr_xFeO_3$ and (b) variation of M_S (M_R in the inset) with Cr concentration for $GaFe_{1-x}Cr_xO_3$ and $Ga_{1-x}Cr_xFeO_3$.

[13]) as implemented in the Vienna *ab initio* Simulation Package (VASP) [14,15]. The projector augmented wave (PAW) method [16] was used to capture interaction between ionic cores and valence electrons. An energy cut off of 400 eV was used in truncation of the plane wave basis and integrations over the Brillouin were carried out using a regular $4 \times 2 \times 2$ mesh of *k*-points. Structure was optimized to minimum energy using Hellman–Feynman forces, while maintaining the lattice constants at their experimental values. Minimum energy states with different magnetic ordering were obtained through appropriate initialization of the spins on Fe and Cr sites.

In simulations of Cr doping at the cation sites, we considered both antiferromagnetic (AFM) (note that this forms a ferrimagnetic (FiM) state with a nonzero moment) and ferromagnetic (FM)

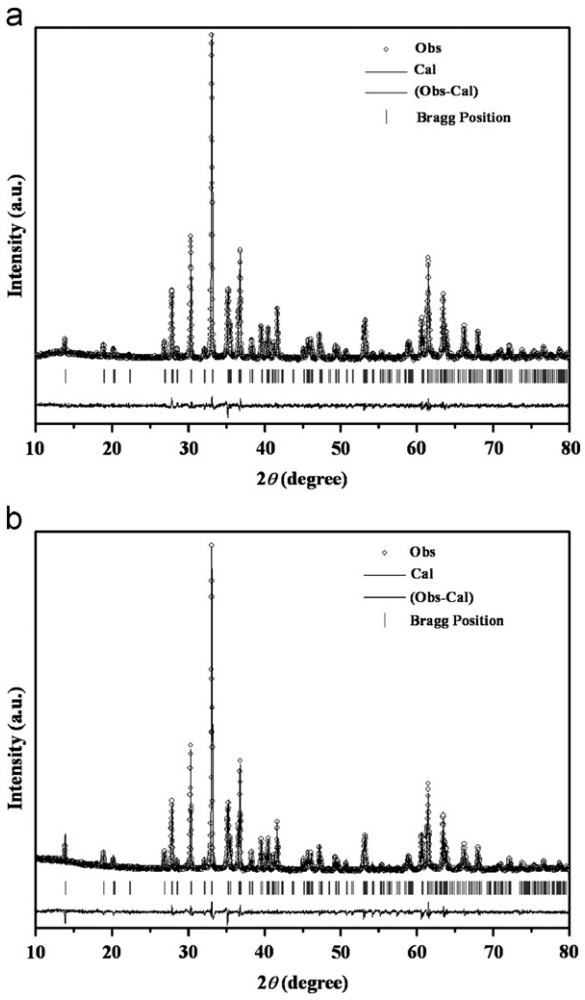

Fig. 6. XRD patterns of (a) $GaFe_{0.9}Mn_{0.1}O_3$ and (b) $Ga_{0.9}Mn_{0.1}FeO_3$ along with profile fits, difference patterns and Bragg positions.

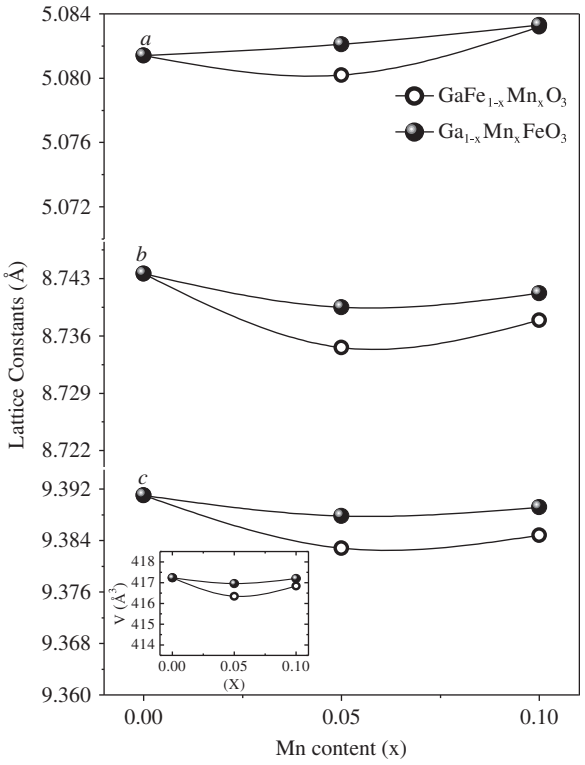

Fig. 7. Variation of lattice constants in $GaFe_{1-x}Mn_xO_3$ and $Ga_{1-x}Mn_xFeO_3$ with Mn content at 300 K obtained from XRD data. Variation of unit cell volume is shown in the inset.

configurations, i.e., magnetic moments on transition metals aligned anti-parallel or parallel to each other [6]. From the cohesive energies of these configurations, we find that Cr doping at Ga2 site with antiferromagnetic ordering of spins is favorable (-6.94 eV/atom). Since both Fe1 and Fe2 sites have octahedral coordination, energies of Cr substitution at these two sites are almost the same (-6.85 eV/atom). Ga1 being a tetrahedral site, Cr^{3+} cannot occupy it. We have calculated the bond valence sums, V, by

$$V = e^{R_o/B} \sum e^{-R_i/B} \quad (1)$$

Here, R_o is the length of a bond of unit valence, R_i is the bond length of bond i the ion is connected to and B is a parameter, approximately equal to 0.37 Å for most bonds [17]. Knowledge of the bond valence sums against the nominal oxidation state of each atom allows one to assess if a given structure obeys the normal rules of structural chemistry. If the bond valence sum differs by more than 0.1 valence unit from the oxidation state of the ion, it suggests that the structure may not be stable. We have used VESTA software [18] and the bond-lengths in the relaxed structure obtained here to carry out bond valence analysis of Cr–O bonds in all the configurations of Cr doping. We have given bond valence sums for the Cr ion at the Fe1, Fe2, Ga1 and Ga2 sites in Table 5. Since Cr is in the 3+ oxidation state, according to the criterion for stability of the structure discussed above, Cr substitution at Ga2 (both AFM and FM states) and Fe1 (both AFM and FM) sites is favoured. On the other hand, Cr is relatively weakly bonded to the lattice when substituted at Fe2 and Ga1 sites. We note that the overall energetics would have contributions from all the ions and bonds giving rise to reasonable stability of all the configurations. However, bond-valence analysis allows us to infer that the structure is not locally stable, particularly at the substituted Cr-site.

Noting that Fe1–O–Fe1 and Fe2–O–Fe2 bond angles are quite smaller than 150° and Fe1–O–Fe2 bond angles are close to 180°, we have focused on magnetic configurations with moments/spins at all Fe1 sites aligned up and those at all Fe2 sites aligned down. Even in the AFM configurations, there is an overall magnetic moment (Table 6) in the system reflecting the asymmetry in the electronic density of states with up and down spins (Fig. 10). This asymmetry, prominent near the Fermi energy, is stronger in the case of Cr substitution at Ga2 site correlating with its larger total magnetic moment. Also, the pseudo gap at the Fermi energy in the Ga2-AFM configuration reaffirms its greater relative stability inferred from bond-valence analysis. Although spins of magnetic ions at all the sites were initialized with the up state, these magnetic moments relax to slightly different spin configurations, particularly the one at Cr-site (Table 6) in the self-consistent solution. The magnetic moment of Cr ion in the AFM (i.e. FiM) case is the largest for doping at the Ga2 site. Cr at the Ga2 site is connected to 4 Fe1 sites via oxygen with (Fe1–O–Cr) bond angles of 165°, 130°, 104° and 99°. Cr^{3+} and Fe^{3+} ions being in the d^3 and d^5, states respectively, super-exchange between Cr and Fe1 connected with a bond angle of 165° is FM in nature, while it is AFM for the remaining Fe1 sites with bond angles of $< 150°$. This leads to the orientation of spin at the Cr substituted at Ga2 site parallel to that of the spins on the Fe1 site (opposite to the Fe2 site) in the former and anti-parallel to the spins on the Fe1 site

Table 4
Results of structure refinement of $Ga_{0.9}Mn_{0.1}FeO_3$ at 300 K.

$Ga_{0.9}Mn_{0.1}FeO_3$ (300 K)					
Space group: $Pna2_1$ (orthorhombic), a=5.0833 (7) Å, b=8.7412 (1) Å, and c=9.3892 (1) Å					
Atoms	x/a	y/b	z/c	B_{iso}	Occ.
Fe1/Ga3	0.1985 (10)	0.1554 (8)	0.5860 (4)	0.33 (11)	0.65 (0)/0.35 (0)
Fe2/Ga4	0.6739 (8)	0.0331 (4)	0.7954 (9)	0.47 (7)	0.70 (0)/0.30 (0)
Ga1/Fe3	0.1722 (8)	0.1488 (7)	0.0000 (0)	0.97 (11)	0.91(0)/0.09 (0)
Ga2/Fe4/Mn	0.8147 (7)	0.1613 (5)	0.3081 (8)	0.48 (9)	0.30 (0)/0.50 (0)/0.20 (0)
O1	1.011 (3)	0.326 (2)	0.422 (1)	0.31 (10)	1.000 (0)
O2	0.518 (3)	0.481 (2)	0.428 (2)	0.31 (10)	1.000 (0)
O3	0.654 (3)	−0.009 (2)	0.203 (1)	0.31 (10)	1.000 (0)
O4	0.159 (3)	0.159 (2)	0.206 (1)	0.31 (10)	1.000 (0)
O5	0.867 (3)	0.162 (2)	0.675 (1)	0.31 (10)	1.000 (0)
O6	0.539 (3)	0.168 (2)	0.940 (1)	0.31 (10)	1.000 (0)
χ^2	2.32%				
R_{Bragg}	7.61%				

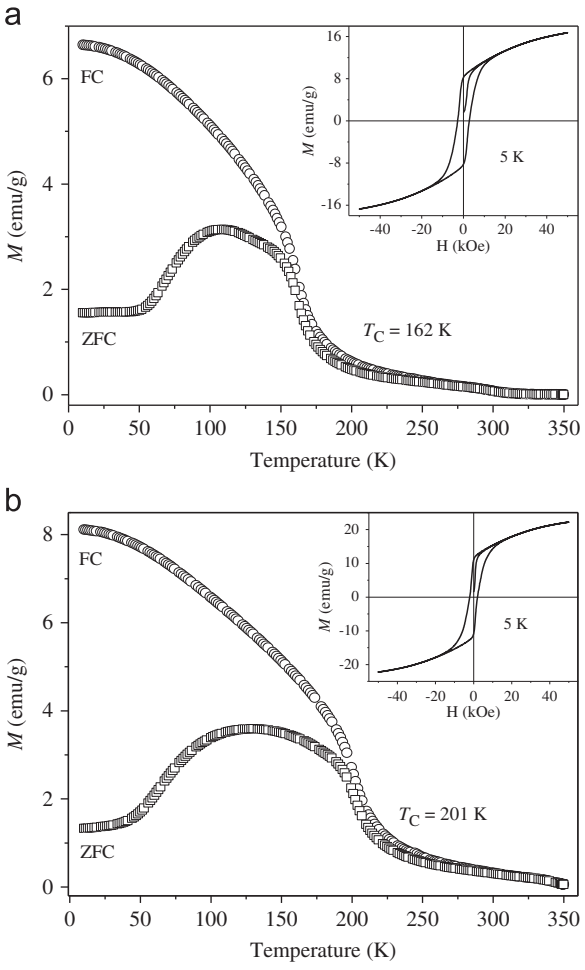

Fig. 8. Temperature-dependent magnetization of (a) $GaFe_{0.9}Mn_{0.1}O_3$and (b) $Ga_{0.9}Mn_{0.1}FeO_3$ under field-cooled (FC) and zero-field-cooled (ZFC) conditions. Magnetic hysteresis at 5 K is shown in the inset.

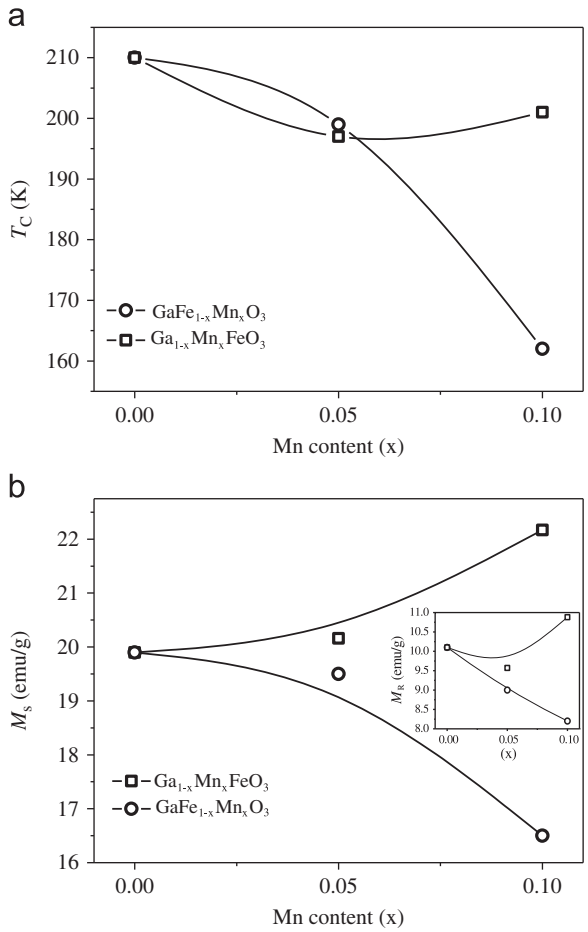

Fig. 9. (a) Variation of the Curie temperature (T_C) with Mn concentration for $GaFe_{1-x}Mn_xO_3$ and $Ga_{1-x}Mn_xFeO_3$ and (b) variation of M_S (M_R in the inset) with Mn concentration for $GaFe_{1-x}Mn_xO_3$ and $Ga_{1-x}Mn_xFeO_3$.

(parallel to the Fe2 site) in the latter. These competing interactions lead to nearly the same energies of configurations with the spin of Cr^{3+} (a) parallel and (b) anti-parallel to the spins at the Fe1 sites. Thus, the AFM (FiM) state and associated transition is not affected much by Cr substitution at the Ga2 site, while maintaining a sizeable magnetic moment of Cr^{3+} (Table 6). In contrast, substitution of Cr at the Fe1 site results in the reduction of the total magnetic moment.

To understand the observed change in T_C with Cr substitution in $GaFeO_3$ requires inclusion of the effects of disorder. Undoped $GaFeO_3$ has anti-site disorder between Ga2 and Fe sites [6]. This disorder is promoted further when Cr is substituted at the Fe1

Table 5
Bond valence sum of Cr–O bonds.

Cation site	Magnetic ordering	
	FM	AFM
Fe1	2.98	3.07
Fe2	3.12	3.22
Ga1	3.30	3.36
Ga2	3.03	3.06 (AFM)[a] 3.003 (FM)[a]

[a] AFM: Fe1–O–Cr AFM interaction; FM: Fe1–O–Cr FM interaction.

Table 6
Total magnetic moment and magnetic moments of Cr^{3+}.

Cation site	Total magnetic moment (μ_B)		Magnetic moment on Cr (μ_B)	
	FM	AFM	FM	AFM
Fe1	23.20	−1.87	2.66	2.39
Fe2	26.01	1.99	2.52	−2.29
Ga1	22.00	1.91	−1.79	1.69
Ga2	20.03	−2.79 (AFM)[a] 2.8 (FM)[a]	2.66	−2.57 (AFM)[a] 2.68 (FM)[a]

[a] AFM: Fe1–O–Cr AFM interaction; FM: Fe1–O–Cr FM interaction.

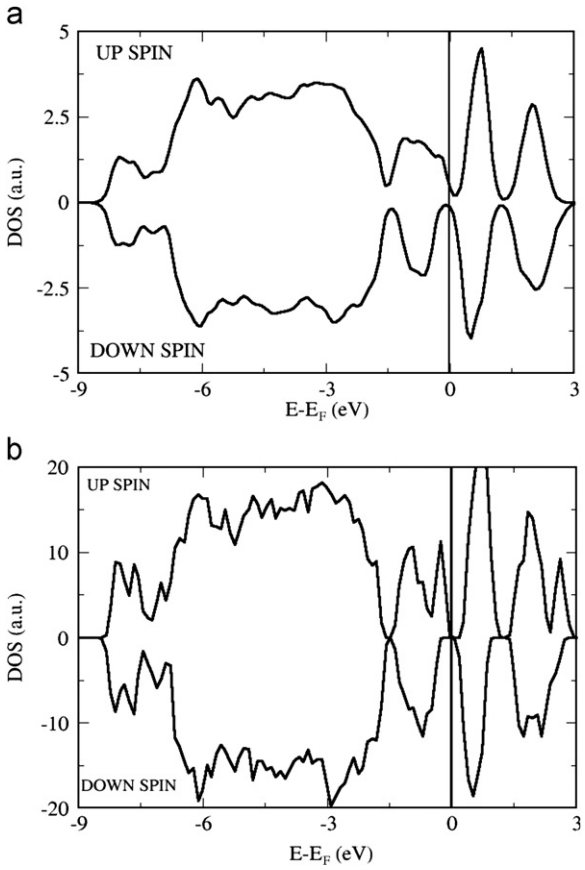

Fig. 10. Electronic density of states for (a) Cr at Ga2 site with AFM ordering and (b) for Cr at Fe1 site with AFM ordering.

site, while it is reduced when Cr is substituted at the Ga2 site. As disorder results in the reduction of the strength of magnetic interactions [6], we expect reduction in T_C when Cr substitution occurs at the Fe1 site. On the other hand, disorder is expected to be weaker when Cr is substituted at the Ga2 sites, and the strength of AFM super-exchange therefore remains roughly the same (while increasing the overall magnetic moment). We, therefore, expect T_C to remain nearly the same for Cr substitution at Ga2 sites as observed in our experiments. Note that in the octahedral coordination, Cr^{3+} ion has an ionic radius of 61.5 pm, whereas Fe^{3+} has an ionic radius of 64.5 pm in the high spin state and 55.0 pm in the low spin state in an octahedral oxygen environment. Ga^{3+} in octahedral (Ga2) and tetrahedral (Ga1) coordination has ionic radii of 62.0 and 47.0 pm, respectively. The difference in ionic radii is the least for Cr at Ga2 site as compared to that of Fe1 or Fe2 sites. We expect compressive stress on the crystal when Cr is substituted at the Fe1 site and hence reduction in unit cell volume and subsequent reduction in the strength of AFM interactions and T_C. In contrast, our simulations reveal no significant stress when Cr is substituted at the Fe2 site (AFM ordering), correlating with essentially no change in T_C in this case.

4. Conclusions

The present study demonstrates how site dependence of the effect of substitution of Cr and Mn ions in $GaFeO_3$ manifests itself and can be delineated starting with suitable oxide precursors preferentially containing Cr (Mn) in the Ga or the Fe site. It is noteworthy that Cr (Mn) substitution in the octahedral Fe (1, 2) site of $GaFeO_3$ has marked effects on the structural parameters and magnetic properties, while substitution in the octahedral Ga2 site has marginal effects. Results obtained with samples prepared by heating all the component oxides together [11,12] fail to distinguish effects of different sites and the observed changes would have contributions from different types of substitution. First-principles calculations clearly demonstrate how substitution of Cr in the octahedral Ga2 and Fe1 sites results in different effects on the unit cell parameters and magnetic properties of $GaFeO_3$. Thus, both experiment and theory confirm the important role of the substitution site in $GaFeO_3$ in determining the effects of Cr (Mn) ions.

References

[1] K. Kelm, W. Mader, Z. Anorg. Allg. Chem. 631 (2005) 2383.
[2] F. Bouree, J.L. Baudour, E. Elbadraoui, J. Musso, C. Laurent, A. Rousset, Acta Crystallogr. B52 (1996) 217.
[3] L.F. Cotica, I.A. Santos, M. Venet, D. Garcia, J.A. Eiras, A.A. Coelho, Solid State Commun. 147 (2008) 123.
[4] R.B. Frankel, N.A. Blum, S. Foner, A.J. Freeman, M. Schieber, Phys. Rev. Lett. 15 (1965) 958.
[5] A. Shireen, R. Saha, P. Mandal, A. Sundaresan, C.N.R. Rao, J. Mater. Chem. 21 (2011) 57.
[6] R. Saha, A. Shireen, A.K. Bera, Sharmila N. Shirodkar, Y. Sundarayya, N. Kalarikkal, S.M. Yusuf, U.V. Waghmare, A. Sundaresan, C.N.R. Rao, J. Solid State Chem. 184 (2011) 494.
[7] H. Wakai, Y. Sinya, A. Yamanaka, Phys. Status Solidi C 8 (2011) 537.
[8] T. Grygar, P. Bezdicka, J. Dedecek, E. Petrovsky, O. Schneeweiss, Ceramics-Silikaty 47 (2003) 32.
[9] J. Lai, K.V.P.M. Shafi, K. Loos, A. Ulman, Y. Lee, T. Vogt, C. Estournes, J. Am. Chem. Soc. 125 (2003) 11470.
[10] H. Hayashi, R. Huang, H. Ikeno, F. Oba, S. Yoshioka, I. Tanaka, S. Sonoda, Appl. Phys. Lett. 89 (2006) 181903.
[11] M.B. Mohamed, H. Wang, H. Fuess, J. Phys. D: Appl. Phys 43 (2010) 455409.
[12] M.B. Mohamed, H. Fuess, J. Magn. Magn. Mater. 323 (2011) 2090.
[13] S.C. Abrahams, J.M. Reddy, J.L. Bernstein, J. Chem. Phys. 42 (1965) 3957.
[14] G. Kresse, J. Hafner, Phys. Rev. B 47 (1993) R558.
[15] G. Kresse, J. Furthmller, Phys. Rev. B 54 (1996) 11 169.
[16] G. Kresse, D. Joubert, Phys. Rev. B 59 (1999) (1758).
[17] 〈http://web.me.com/willsas/Site/Bond valence calculations %3 A guide. html〉.
[18] K. Momma, F. Izumi, J. Appl. Crystallogr. 41 (2008) 653.